Gynecologic Oncology 152 (2019) 618–628

Contents lists available at ScienceDirect

Gynecologic Oncology

journal homepage: www.elsevier.com/locate/ygyno

MUC16 suppresses human and murine innate immune responses

Mildred Felder [a], Arvinder Kapur [a], Alexander L. Rakhmilevich [b], Xiaoyi Qu [b], Paul M. Sondel [c], Stephen D. Gillies [d], Joseph Connor [e,*], Manish S. Patankar [a,**]

[a] Department of Obstetrics and Gynecology, University of Wisconsin, Madison, WI, USA
[b] Department of Human Oncology, University of Wisconsin, Madison, WI, USA
[c] Departments of Pediatrics and Human Oncology, University of Wisconsin, Madison, WI, USA
[d] Provenance Biopharmaceuticals, Carlisle, MA, USA
[e] Department of Pathology and Laboratory Medicine, University of Wisconsin, Madison, WI 53792, USA

HIGHLIGHTS

- The mucin MUC16 carries the peptide epitope that defines the biomarker CA125.
- We provide data supporting the immunosuppressive effects of MUC16.
- MUC16 prevents human immune cells from conjugating with ovarian cancer cells.
- MUC16 also inhibits the cytolytic responses of murine NK and macrophages.
- Studies on MUC16 in murine models should consider the suppressive effects of MUC16 on murine immune cells.

ARTICLE INFO

Article history:
Received 17 October 2018
Received in revised form 18 December 2018
Accepted 26 December 2018
Available online 6 January 2019

Keywords:
Immunesuppression
MUC16
CA125
NK cells
Ovarian cancer
Antibody-mediated cytotoxicity
Immune evasion

ABSTRACT

Objective. MUC16, the mucin that contains the CA125 epitopes, suppresses the cytolytic responses of human NK cells and inhibits the efficacy of therapeutic antibodies. Here, we provide further evidence of the regulatory role of MUC16 on human and murine NK cells and macrophages.

Methods. Target cell cytolysis and doublet formation assays were performed to assess effects of MUC16 on human NK cells. The effect of MUC16 on ovarian tumor growth was determined in a mouse model by monitoring survival and ascites formation. Innate immune cells from spleens and peritoneal cavities of mice were isolated and stimulated *in vitro* with anti-CD40 antibody, lipopolysaccharide and IFN-γ and their ability to cytolyse MUC16 expressing and non-expressing cells was determined.

Results. We confirm that MUC16 inhibits cytolysis by human NK cells as well as the formation of NK-tumor conjugates. Mice implanted with MUC16-knockdown OVCAR-3 show >2-fold increase in survival compared to controls. Murine NK cells and macrophages are more efficient at lysing MUC16-knockdown cells. *In vitro* cytotoxicity assays with NK cells and macrophages isolated from mice stimulated with anti-CD40 antibody showed 2–3-fold increased activity against the MUC16-knockdown cells as compared to matching target cells expressing this mucin. Finally, knockdown of MUC16 increased the susceptibility of cancer cells to ADCC by murine splenocytes.

Conclusions. For the first time, we demonstrate the immunoregulatory effects of MUC16 on murine NK cells and macrophages. Our study implies that the immunoregulatory role of MUC16 on murine NK cells and macrophages should be considered when examining the biology of MUC16 in mouse models.

1. Introduction

The biomarker CA125 is used to monitor progression of high grade serous ovarian cancer [1]. CA125 is a repeating peptide epitope of the 3–5 million Da membrane-spanning mucin, MUC16 [2,3]. While the majority of CA125 research over the past 3–4 decades has focused on its biomarker potential, only recently has there been progress in understanding the biological role of MUC16 in normal tissues and tumors. Studies with ovarian, breast and pancreatic cancer cell lines and

* Correspondence to: J.P. Connor, Department of Pathology, University of Wisconsin-Madison, 600 Highland Avenue, H4/654 CSC, Madison, WI 53792, USA.
** Correspondence to: M.S. Patankar, Department of Obstetrics and Gynecology, University of Wisconsin-Madison, 600 Highland Avenue, H4/654 CSC, Madison, WI 53792, USA.
E-mail addresses: jconnor@uwhealth.org (J. Connor), patankar@wisc.edu (M.S. Patankar).

https://doi.org/10.1016/j.ygyno.2018.12.023
0090-8258/

in vivo models have indicated that MUC16 promotes cancer cell proliferation and metastasis and may also contribute to chemoresistance [4–10]. MUC16 also protects ovarian and breast cancer cells from cytolysis by human natural killer (NK) cells [11–14].

MUC16 is a transmembrane mucin that is cleaved from the cell surface [1,15]. Several reports have demonstrated the immunomodulatory roles of both the membrane-bound and the cleaved forms of MUC16 [12–14,16–20]. Our group was the first to show that pre-incubation with shed MUC16 inhibited the cytolytic activity of human NK cells [12]. Further analysis showed that MUC16 is a ligand of Siglec-9, a human ITIM-containing inhibitory receptor expressed on most monocytes, approximately 40% of NK cells and some T cell subsets [13]. In ocular epithelia, MUC16 serves as a barrier to bacterial adherence and a similar mechanism may also contribute to this mucin's ability to attenuate interactions between tumor cells and immune cells [21]. In this context, it is interesting to note that tumor cells engineered to express truncated O-glycan chains on MUC16 (due to knockdown of the molecular chaperon COSMC) are significantly more susceptible to ADCC and antigen-specific killing by cytolytic T cells [16].

Recent reports from a clinical trial of the anti-folate receptor antibody, farletuzumab, and the anti-mesothelin antibody, amatuximab, show that patients with lower serum CA125 levels showed improved overall and progression free survival [18–20]. The decreased effect of farletuzumab and amatuximab in patients with high serum CA125 is attributed to the ability of MUC16 to bind to the $F(ab')_2$ domain of the therapeutic antibody and thereby perturb the interaction of the Fc domain with the Fc-γ receptor on immune cells [18–20]. Evidence exists that the mucin interacts with the $F(ab')_2$ domain of rituximab, gimsilumab, and other therapeutic antibodies as well [18].

All of these previous observations indicate that MUC16 could serve as a barrier to natural immune cytotoxicity as well as to immunotherapy against tumors. We posit that extensive studies will be needed to understand the immunomodulatory role of MUC16. Such studies will need to delineate the role of cell bound and shed MUC16 and, at the molecular level, identify peptide as well as glycan epitopes of the mucin that interact with immune cell receptors. The molecular complexity of MUC16 is a formidable barrier to studying its immunologic role, but the development of modern gene editing techniques makes it possible to express epitopes of MUC16 in tumor cells of human as well as mouse origin, thereby aiding researchers in this area of investigation.

In vivo studies in mouse models will be useful in understanding the immunobiology of MUC16. At the current time, although a collection of studies has demonstrated several effects of MUC16 on human immune cells, there is no systematic study demonstrating that this mucin can also inhibit murine immune responses. This deficiency in our understanding is addressed in the current study. Here, we demonstrate that MUC16-expressing tumors are protected from cytolytic responses of murine NK cells and macrophages. Our findings show that MUC16-mediated protection of target cells is observed even when the murine immune cells are activated with anti-CD40 antibody or lipopolysaccharides. The strong protective effects demonstrated here provide a foundation for future exploration of the immunosuppressive effects of MUC16 using appropriate murine models.

2. Materials and methods

2.1. Cell lines and reagents

SCID, SCID/Beige, and C57BL/6 mice were purchased from Harlan Laboratories (Madison, WI). Blood collection from healthy donors was approved by the Institutional Review Board (protocol number 2015-1403). The experiments with mice were approved by the Institutional Animal Care and Use committee (protocol number M005763). Peripheral blood mononuclear cells (PBMC) were isolated by density gradient centrifugation using Ficoll-Paque Plus (GE Healthcare Life Sciences, Piscataway, NJ). The parent OVCAR-3 and B16 cell lines were obtained from ATCC (Manassas, VA). Cell culture media (RPMI 1640 supplemented with 20% fetal bovine serum, sodium bicarbonate, sodium pyruvate, HEPES, insulin, glucose and penicillin/streptomycin) was purchased from Mediatech (Manassas, VA) and antibodies for flow cytometry were purchased from BD Biosciences (San Diego, CA) unless noted otherwise. All other reagents were from ThermoFisher, MA.

2.2. MUC16 knockdown

Development of stable OVCAR-3 clones expressing either an endoplasmic reticulum localized scFv fragment of the anti-MUC16 antibody VK8 (OV-MUC16$^{scFv\text{-}KD}$) or a non-specific mouse IgG antibody (OV-MUC16$^{scFv\text{-}ctrl}$) has been previously described [7,22]. MUC16 expression on these cells was routinely monitored by flow cytometry.

2.3. In vivo studies

Six-week old female SCID and SCID/Beige mice were housed in an aseptic animal care facility. The OV-MUC16$^{scFv\text{-}ctrl}$ and OV-MUC16$^{scFv\text{-}KD}$ cells (20×10^6) were injected intraperitoneally on day 0 of the experiment. Body weights of the tumor-bearing animals were recorded every week. All animals were also monitored for adverse physical symptoms, development of palpable tumors, and ascites accumulation. Mice that became moribund or those that had to be further investigated for experimental considerations were euthanized by CO_2 asphyxiation. A peritoneal tap was used to collect ascites and the animals were necropsied to locate tumors and obtain tissues for immunohistochemistry.

2.4. Immunohistochemical analysis

Tumors were excised from mice at time of euthanasia and cryopreserved. Five μm sections of the tumors were made on a cryostat. Consecutive slides obtained from a single tumor specimen were stained with hematoxylin and eosin or incubated with anti-F4/80 antibody (eBioscience, San Diego, CA) and developed with the Vectastain Elite ABC peroxidase and DAB kits from Vector Labs (Burlingame, CA) to identify macrophages. A non-specific rat IgG2a (purchased from BD Biosciences, CA) was tested for background staining and found to be no different from antibody diluent alone; thereafter, antibody diluent was used for the negative control sections.

2.5. Cell proliferation assay

Cancer cells were plated in a 96-well plate (5,000 cells/well) for 24, 72 and 96 h in cell culture media. After incubation, the media was removed and each well was carefully washed with phosphate buffered saline (PBS). Calcein AM (1 μg/ml in PBS) was added to each well (200 μl/well) and the cells were incubated at room temperature for 2 h. The staining solution was removed and each well was washed with PBS and the fluorescence in each well was measured using a microplate reader (505 excitation/530 emission). To account for background fluorescence, in each experiment the calcein AM was added to empty (no cells) wells. The wells were treated the same way as the wells that contained the cancer cells. The fluorescence from these empty wells was measured and the average background fluorescence units were calculated. This average was subtracted from the fluorescence measured for each of the test wells and the data was plotted using GraphPad Prism software package. To obtain robust data three biological replicates were included. Thirty technical replicates were included in each biological repeat. An unpaired *t*-test was used for statistical analysis of the data set.

2.6. Flow cytometry analysis

MUC16, EpCAM and HLA-ABC expression on ovarian cancer cells were measured by flow cytometry, with MUC16 being monitored

using the antibody produced by the VK8 hybridoma (kindly provided by Dr. Beatrice Yin, Memorial Sloan Kettering, NY). HLA-ABC expression was monitored with the W6/32 antibody, while EpCAM expression was monitored using the KS1/4 antibody as described earlier [23]. Either PE-labeled goat anti-mouse or APC-labeled donkey anti-mouse (eBioscience) secondary antibodies were used to detect the binding of the primary antibodies. The cells were analyzed on either a FACSCalibur or an LSR-II (BD Biosciences) flow cytometer and the data were analyzed using FlowJo software (Tree Star, Inc. Ashland, OR). Secondary antibody alone was used as the negative control.

2.7. Cell conjugation assay

MUC16-expressing and non-expressing ovarian cancer targets (OVCAR-3, OVCAR-5, OV-MUC16$^{scFv\text{-}KD}$ and OV-MUC16$^{scFv\text{-}ctrl}$) were labeled with CFSE and mixed at a 1:1 ratio with CellTracker Deep Red-labeled human NK leukemia cell line, NKL or human PBMC. In some experiments, the effector and target cells were incubated in the presence of the anti-EpCAM immunocytokine, IC65. This immunocytokine was developed and purified using a previously reported protocol [24]. After a gentle centrifugation (2 min at 100 ×*g*), the cells were incubated for 40 min at 37 °C, PI was added with minimal perturbation and cells were analyzed by flow cytometry for live (PI negative) doublets having both CFSE and CellTracker Deep Red dye labels.

2.8. In vivo stimulation with anti-CD40 antibody

Female eight to12-week old C57BL/6 or SCID mice were injected intraperitoneally with 0.5 mg anti-CD40 antibody produced by the FGK45.5 hybridoma. Three days after administration of the anti-CD40 antibody, animals were euthanized and the spleens were removed to obtain murine effector cells. In some cases, peritoneal exudate cells (PEC) were also obtained by peritoneal cavity lavage.

2.9. Cytotoxicity assays

To determine the ability of murine NK cells to lyse human ovarian cancer cell targets, splenocytes were isolated from female C57BL/6 or SCID mice. Immediately after harvest, spleens were dissociated in cold PBS and the resulting cellular suspension was passed over a 70 μM strainer. Following centrifugation, the red blood cells were lysed by hypotonic shock and the remaining intact immune cells were washed and pelleted by centrifugation. Splenocytes were then counted and diluted to the appropriate concentration in complete medium (RPMI supplemented with L-glutamine, penicillin, streptomycin and 10% FBS).

For enrichment of NK cells, splenocytes were resuspended in MACS buffer and prepared according to manufacturer's recommendations. Briefly, cells were incubated for 5 min at 4 °C with the Biotin-Antibody Cocktail from the mouse NK Cell Isolation Kit II (Miltenyi Biotec, Auburn, CA), washed and resuspended in MACS buffer with Anti-Biotin Microbeads and incubated a further 10 min at 4 °C. After adjusting the volume according to number of cells per tube, the splenocytes were separated into NK-enriched and NK-diminished/depleted populations with the depletion program on the autoMACS Pro Separator (Miltenyi Biotec, Auburn, CA). A sufficient number of cells for flow cytometry were removed from the pre- and post-sorted populations and the remaining cells were plated for cytotoxicity assays as already described. Although the MACS cell separation method employed was optimized for C57BL/6 splenocytes, we observed that the enriched population contained approximately 37% of the NKp46^{+} NK cells. In comparison, the total splenocyte pool prior to cell separation on MACS contained on average only 25% of the NKp46^{+} NK cells.

PEC were washed and resuspended in complete medium at a concentration of 2×10^6/ml. After plating 100 μl/well in flat-bottomed 96-well plates, the PEC population was enriched for macrophages by allowing the cells to adhere for 1.5 h, then washing thrice with medium to remove non-adherent cells. For the assays in which they were used, IFN-γ (R&D Systems, Minneapolis, MN), LPS (Sigma-Aldrich, St. Louis, MO), and KSIL-2 were added at indicated concentrations just prior to adding the tumor targets.

Tumor targets were labeled with ^{51}Cr using a standard protocol [25]. Labeled targets (5,000 cells/well) were mixed with either mouse splenocytes, mouse macrophages, or human peripheral blood mononuclear cells at appropriate effector:target cell ratios and incubated at 37 °C and 5% CO_2. For the NK cell cytotoxicity assays, effectors and target cells were co-incubated for 4 h while for the macrophage assays, the co-incubation was for 19 h. After incubation, the supernatant was harvested and ^{51}Cr released from target cells was counted on a Packard gamma-counter.

2.10. Cytostatic effect of macrophages

Cytostatic activity of mouse macrophages against tumor cell lines was determined by the inhibition of DNA synthesis in target tumor cells. PEC were obtained and prepared as described above, then indicated tumor cells (10^4/well) and treatments or controls were added and co-cultured for 72 h. During the last 6 h of incubation, cells were pulsed with [^{3}H]-thymidine (1 μCi/well), then harvested onto glass fiber filters which were allowed to dry overnight. [^{3}H]-thymidine incorporation as a measure of tumor cell proliferation was determined by β-scintillation of total cells harvested (macrophage [^{3}H]-thymidine incorporation is negligible) using the Packard Matrix 9600 Direct Beta Counter (Packard Instrument, Meriden, CT). Results are expressed as counts per 5 min for triplicate wells ±SEM. We have previously established that inhibition of tumor cell proliferation by adherent PEC in this assay is due to macrophages [26].

3. Results

3.1. MUC16 prevents interaction between innate immune cells and tumor cells

Previously we have shown that MUC16 inhibits the formation of immune synapses between human NK cells and cancer cells [14]. To further support our prior observations, we developed a flow cytometry assay to demonstrate that MUC16 inhibits interactions between tumor cells and human NK cells. MUC16-expressing OVCAR-3 cells and MUC16-negative OVCAR-5 cells (Fig. 1A) were labeled with CFSE and mixed at a 1:1 ratio with Celltracker Deep Red-labeled human NK cell leukemia cell line, NKL. When the doublet events were gated, approximately 9% of all live cells were found to be engaged in heterotypic (OVCAR-5-NKL) doublet formation (Fig. 1B). In comparison only minimal (~3%) doublet formation was found between NKL cells and the MUC16-expressing OVCAR-3 cells (Fig. 1B). The increased numbers of doublets with OVCAR-5 cells were observed even though the expression level of HLA class I antigens was higher on these cells as compared to OVCAR-3 cells (Fig. 1C).

Next, we confirmed that MUC16 also prevented ovarian cancer cell from being recognized by primary innate immune cells obtained from healthy human donors. We conducted effector cell-cancer cell conjugation experiments with OVCAR-3-derived cells where MUC16 was knocked down by expressing an endoplasmic reticulum-localized single chain antibody fragment of the anti-MUC16 monoclonal antibody, VK-8 [7,27]. Knockdown of MUC16 on the VK8 scFv expressing OVCAR-3 cell clones (OV-MUC16$^{scFv\text{-}KD}$) was confirmed by flow cytometry (Fig. 2A). OVCAR-3 cells expressing intracytoplasmic scFv of an irrelevant antibody (OV-MUC16$^{scFv\text{-}ctrl}$) were used as MUC16-expressing controls (Fig. 2A).

PBMC isolated from healthy donors (n = 3) were stained with Cell Tracker-Deep Red. When analyzed by flow cytometry, we observed two populations of PBMC- those with lower and higher level of labeling

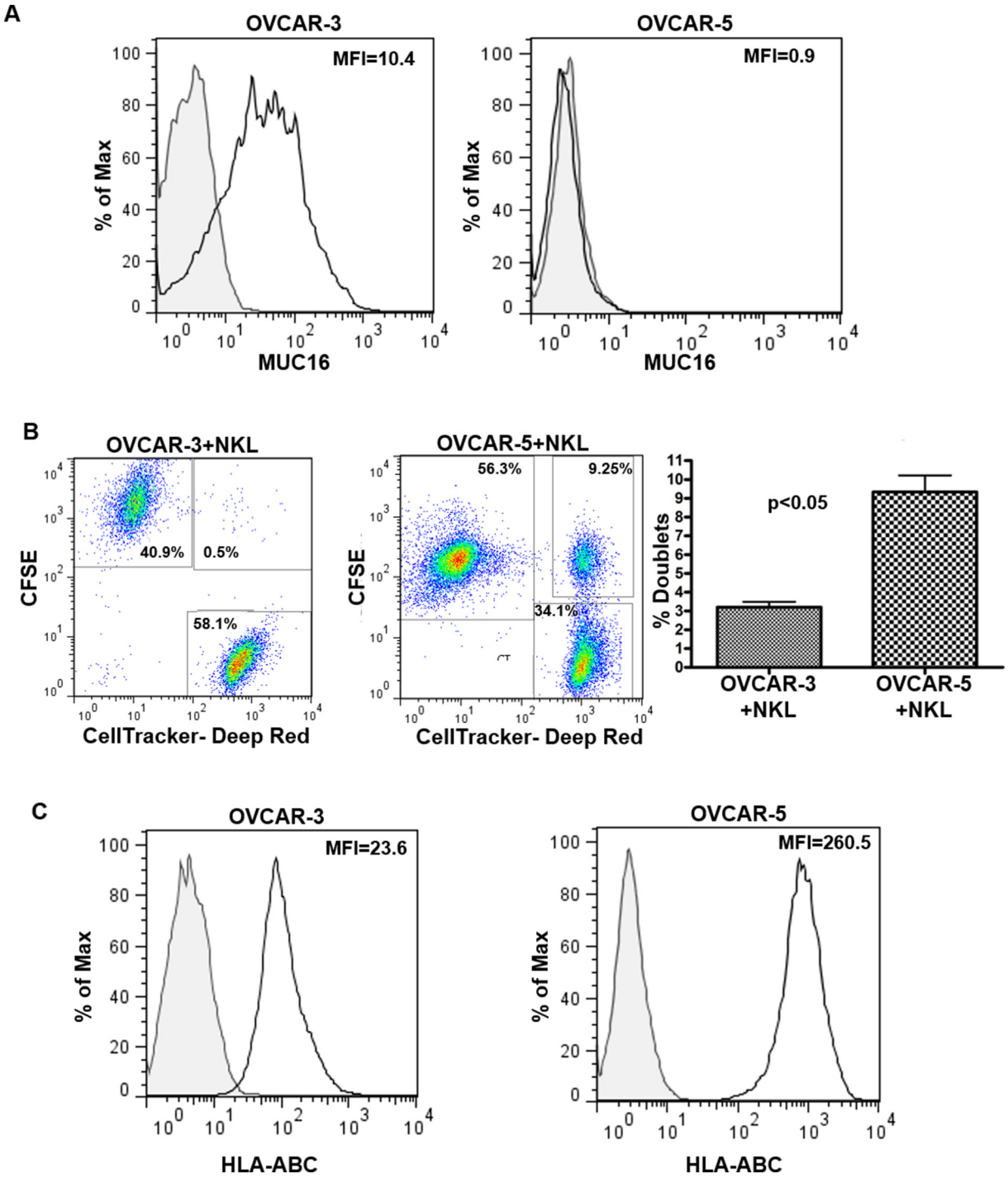

Fig. 1. MUC16 prevents conjugate formation between NKL cells and cancer targets. A: Expression of MUC16 on OVCAR-3 and OVCAR-5 cells was determined by flow cytometry. The cells were labeled with the anti-MUC16, VK8 antibody and binding of the primary antibody was monitored using a PE-labeled goat anti-mouse secondary antibody. The mean fluorescence intensity (MFI) was determined and compared to identify the level of MUC16 present on the surface of the two ovarian cancer cell lines. B: CFSE-labeled OVCAR-3 or OVCAR-5 cells were co-incubated with Celltracker Deep Red-labeled NKL cells for 40 min. The cells were then analyzed by flow cytometry. Dead cells were excluded, then singlet and doublet events were gated as shown. The data shown is representative of three independent replicates. Cumulative data from the three biological replicates is shown in the bar graph. C: Expression of HLA Class I on OVCAR-3 and OVCAR-5 was determined by flow cytometry. Expression of these antigens was monitored on OVCAR-3 and OVCAR-5 cells from different passages and was found to be consistent with that shown here.

with the Cell Tracker-Deep red dye (Fig. 2B and C). Both populations of dye-labeled PBMC contained NK cells and monocytes (data not shown).

Using the doublet formation assay, we observed increased number of doublets with human PBMC when the OV-MUC16$^{scFv\text{-}KD}$ were used as targets as compared to the OV-MUC16$^{scFv\text{-}ctrl}$ cells (Fig. 2B). The increase in doublet formation was observed irrespective of the extent of labeling of the PBMC with the Cell Tracker Deep Red (Fig. 2B). Additionally, the increase in doublet formation between labeled PBMC and the OV-MUC16$^{scFv\text{-}KD}$ cells was also observed in the presence of IC65 (Fig. 2C), an EpCAM targeting immunocytokine. These experiments further support the hypothesis that MUC16 helps tumor cells evade recognition by human immune cells. Confirmation of these immunomodulatory effects

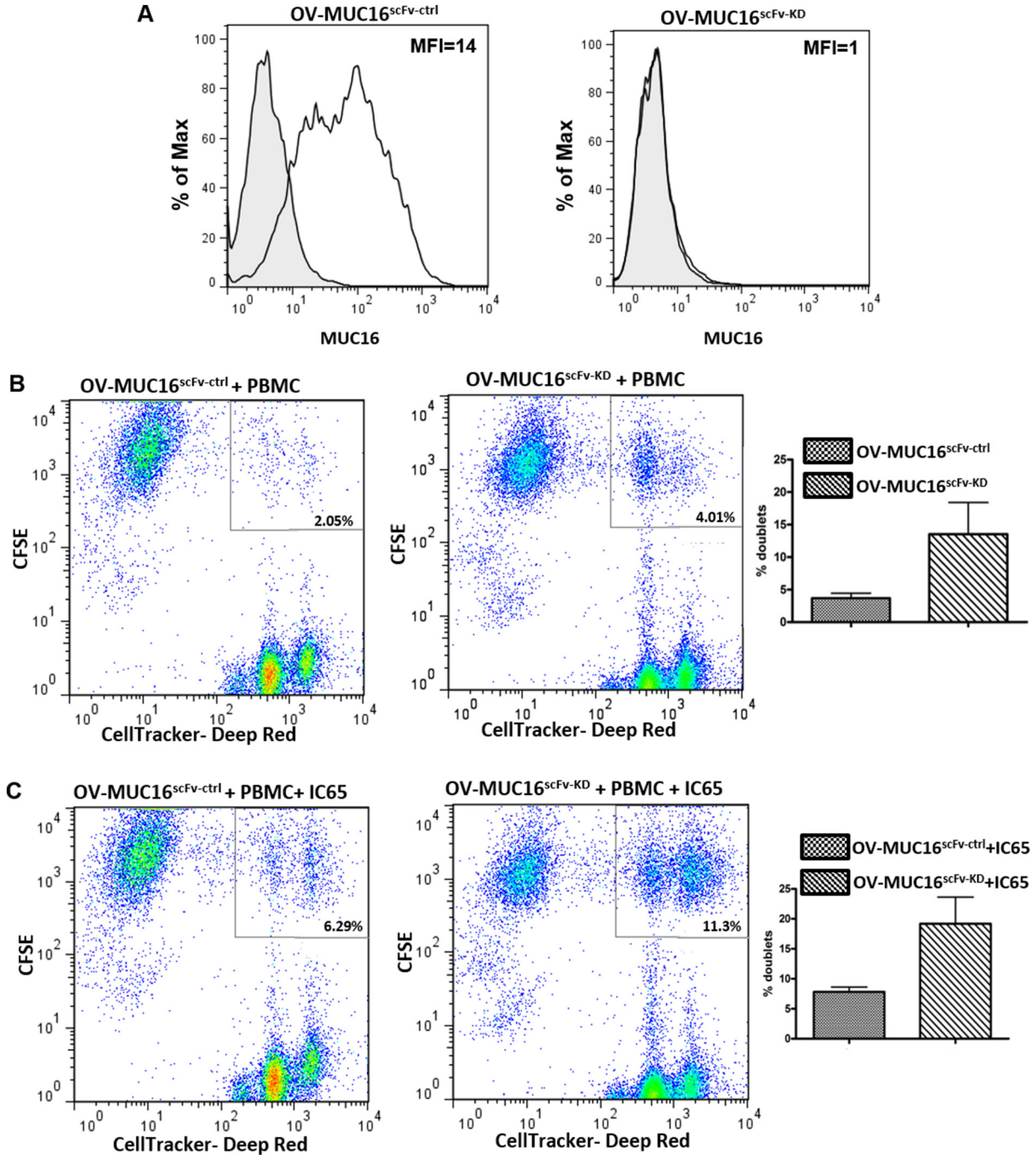

Fig. 2. MUC16 inhibits conjugation between human PBMC and ovarian cancer cells. A: Expression of MUC16 on OV-MUC16$^{scFv\text{-}ctrl}$ and OV-MUC16$^{scFv\text{-}KD}$ cells was monitored by flow cytometry. VK8 was used as the primary antibody and PE-conjugated goat anti-mouse secondary antibody was used for detection. B: CFSE-labeled OV-MUC16$^{scFv\text{-}ctrl}$ and OV-MUC16$^{scFv\text{-}KD}$ co-incubated with PBMC from healthy human donors that were pre-stained with Cell Tracker Deep Red. C: PBMC-target cell conjugation assays were also conducted in the presence of 1 μg/ml of the anti-EpCAM immunocytokine, IC65. Conjugate formation between effectors and cancer targets was monitored by flow cytometry. The low and high level of labeling of the PBMC with Cell Tracker Deep Red resulted in the detection of the two effector cell populations in B and C. The dot plots in B and C are representative results using PBMC from one of three blood donors. The bar graphs in B and C represent average percent doublet formation between PBMC from the three healthy blood donors and the ovarian cancer target cells. The average data in the bar graphs shows trends of increased doublet formation with OV-MUC16$^{scFv\text{-}KD}$ cells as compared to the OV-MUC16$^{scFv\text{-}ctrl}$ targets. However, because of the natural variation in the extent of doublet formation for each PBMC donor, the average data shown in the bar graph is not statistically significant.

of MUC16 led us to determine whether murine models can serve as an important avenue to study the immunoregulatory role(s) of MUC16 *in vivo*.

3.2. MUC16 knockdown increases survival of tumor bearing mice

The tumor-promoting effects of MUC16 are evident from our *in vivo* experiments where OV-MUC16$^{scFv\text{-}KD}$ and OV-MUC16$^{scFv\text{-}ctrl}$ cells were peritoneally implanted in SCID and SCID/Beige mice. First, we demonstrate that the *in vitro* proliferation rates of OV-MUC16$^{scFv\text{-}ctrl}$ and OV-MUC16$^{scFv\text{-}KD}$ cells are not statistically different from each other (Fig. 3A). When implanted in the peritoneum of SCID and SCID/Beige mice, the OV-MUC16$^{scFv\text{-}ctrl}$ cells developed tumors that resulted in a significant increase in the body weight of the animals as well as the development of ascites in the majority of the animals (Fig. 3B–D). These results were in contrast to the mice implanted with the OV-

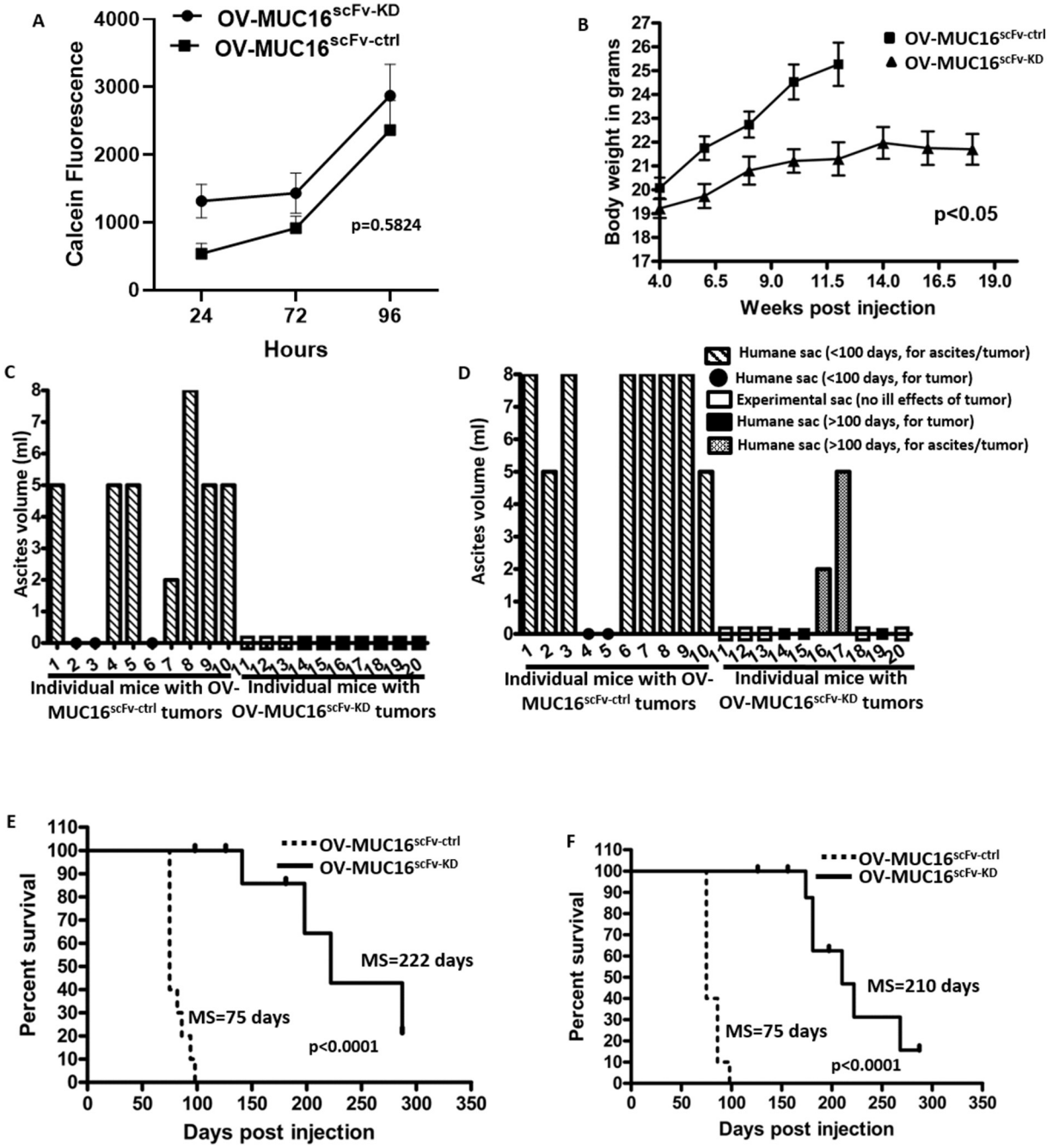

Fig. 3. MUC16 knockdown increases survival of tumor-bearing mice. A: *In vitro* proliferation of OV-MUC16$^{scFv\text{-}ctrl}$ and OV-MUC16$^{scFv\text{-}KD}$ cells was determined by culturing the cells for the designated timepoints. At the end of the experiment, cells were stained with calcein AM and fluorescence in each well was determined to quantify the number of viable cells in each culture. The background fluorescence was subtracted from each datapoint before plotting the graph. The data shown for each timepoint is a mean of thirty technical replicates and is representative of three independent experiments. Unpaired *t*-test was used for statistical analysis. B: OV-MUC16$^{scFv\text{-}ctrl}$ and OV-MUC16$^{scFv\text{-}KD}$ (20×10^6) cells were implanted in the peritoneal cavities of SCID or SCID/Beige mice (10 animals/cell line). Increase in body weight of the tumor-bearing SCID mice was plotted and comparison of the data shows an increased weight gain in mice receiving OV-MUC16$^{scFv\text{-}ctrl}$ tumors. C and D: Volume of ascites recovered from the tumor-bearing SCID (C) and SCID/Beige (D) mice was measured as a surrogate to determining the proliferation of the intraperitoneal tumors. The bars represents the volume of ascites recovered from each tumor-bearing mouse. The legend for the plots describes the reason why the animals were sacrificed and the days after tumor implantation when the terminal procedure was performed. Humane sac was either because of high tumor burden or because of both high tumor volume as well as high volume of ascites that caused significant discomfort to the mice. Some animals (3/10 from the SCID group and 5/10 from the SCID-Beige group) implanted with OV-MUC16$^{scFv\text{-}KD}$ tumors did not show any signs of tumor development upon examination of body conditions and were therefore sacrificed (Experimental Sac) to determine their tumor burden. E and F: Kaplan-Meier survival plots for OV-MUC16$^{scFv\text{-}ctrl}$ and OV-MUC16$^{scFv\text{-}KD}$ tumor-bearing SCID (E) or SCID/Beige (F) mice are shown. Median survival of mice with OV-MUC16$^{scFv\text{-}ctrl}$ or OV-MUC16$^{scFv\text{-}KD}$ tumors is provided in each plot. The difference in the survival of the two cohorts in the SCID as well as SCID/Beige animals was highly significant with a $p < 0.0001$.

MUC16$^{scFv\text{-}KD}$ cells, where the weight gain was lower than in mice with OV-MUC16$^{scFv\text{-}ctrl}$ tumors (Fig. 3B). Furthermore, none of the tumor-bearing SCID (Fig. 3C) and only two of the tumor-bearing SCID/Beige animals (Fig. 3D) developed ascites. The most striking demonstration of the role of MUC16 in promoting tumor growth can be observed in the survival plots, where the SCID and SCID/Beige animals implanted with OV-MUC16$^{scFv\text{-}KD}$ had a median survival of 222 and 210 days, respectively (Fig. 3E and F). In comparison, the median survival of SCID and SCID/Beige mice implanted with OV-MUC16$^{scFv\text{-}ctrl}$ tumors was 75 days (Fig. 3E and F).

3.3. MUC16 inhibits cytolytic responses of naïve and activated murine NK cells

Evidence that MUC16 was also influencing the murine immune responses came from immunohistology of the OV-MUC16$^{scFv\text{-}KD}$ and OV-MUC16$^{scFv\text{-}ctrl}$ tumors excised from the SCID/Beige animals. OV-MUC16$^{scFv\text{-}KD}$ tumors from SCID/Beige animals showed tumoral infiltration by macrophages (Supplementary File 1). In contrast, macrophage infiltration in SCID/Beige mice with OV-MUC16$^{scFv\text{-}ctrl}$ tumors was confined primarily to the tumoral stroma (Supplementary File 1).

These initial observations led us to directly assess the effect of MUC16 on murine NK cells and macrophages in *in vitro* assays. Naïve human NK cells lysed OV-MUC16$^{scFv\text{-}KD}$ cells with significantly higher efficiency than they lysed OV-MUC16$^{scFv\text{-}ctrl}$ cells (Fig. 4A). To test if MUC16 can also suppress murine immune cell responses, we conducted *in vitro* cytolytic assays with murine effector cells against these same tumor target populations. First, splenocytes from immunocompetent C57BL/6 mice were tested in cytolysis assays that measure the lytic activity of NK cells. Splenocytes were obtained three days after the animals were stimulated *in vivo* with the agonistic anti-CD40 antibody, FGK45.5. This anti-CD40 stimulation strategy was adopted because of its demonstrated ability to activate macrophages and NK cells [28] and also its *in vivo* anti-tumor immunotherapeutic activity [29].

The cytotoxicity assays demonstrated that even though the extent of lysis of the targets was relatively low (between 5 and 10%), there was a significant increase in the lysis of the OV-MUC16$^{scFv\text{-}KD}$ (average lysis approximately 7%) over the OV-MUC16$^{scFv\text{-}ctrl}$ cells (average lysis approximately 3–4%, Fig. 4B).

Next, we tested if splenocytes from SCID mice (the mouse model most likely to be used in future studies investigating the *in vivo* immunosuppressive roles of MUC16) were also able to lyse MUC16-knockdown cells with greater efficiency than the MUC16 expressing ovarian cancer cells. Three days prior to the cytolytic assay, SCID mice were stimulated with either anti-CD40 antibody or a non-specific rat IgG. Splenocytes from SCID mice treated *in vivo* with anti-CD40 antibody showed higher level of cytotoxicity when tested in *ex vivo* cytotoxicity assays (Fig. 4C). When compared to the OV-MUC16$^{scFv\text{-}ctrl}$ cells, a 3-fold increase in the lysis of the OV-MUC16$^{scFv\text{-}KD}$ targets by these activated splenocytes was observed (Fig. 4C).

Lipopolysaccharide (LPS) activates the cytolytic responses of murine NK cells [30]. Even in assays where the splenocytes were additionally activated *in vitro* with LPS, a significant increase in the lysis of OV-MUC16$^{scFv\text{-}KD}$ targets was maintained (Fig. 4C), suggesting that the presence of the mucin was sufficient to suppress lytic function even in activated murine NK cells.

The cytolysis of ovarian tumor cell targets observed in these experiments using SCID splenocytes was predominantly due to the resident NK cells as determined by NK cell enrichment and depletion experiments (Fig. 4D). A higher level of cytotoxicity was observed when NK cells were enriched from the SCID splenocytes. The enriched NK cells

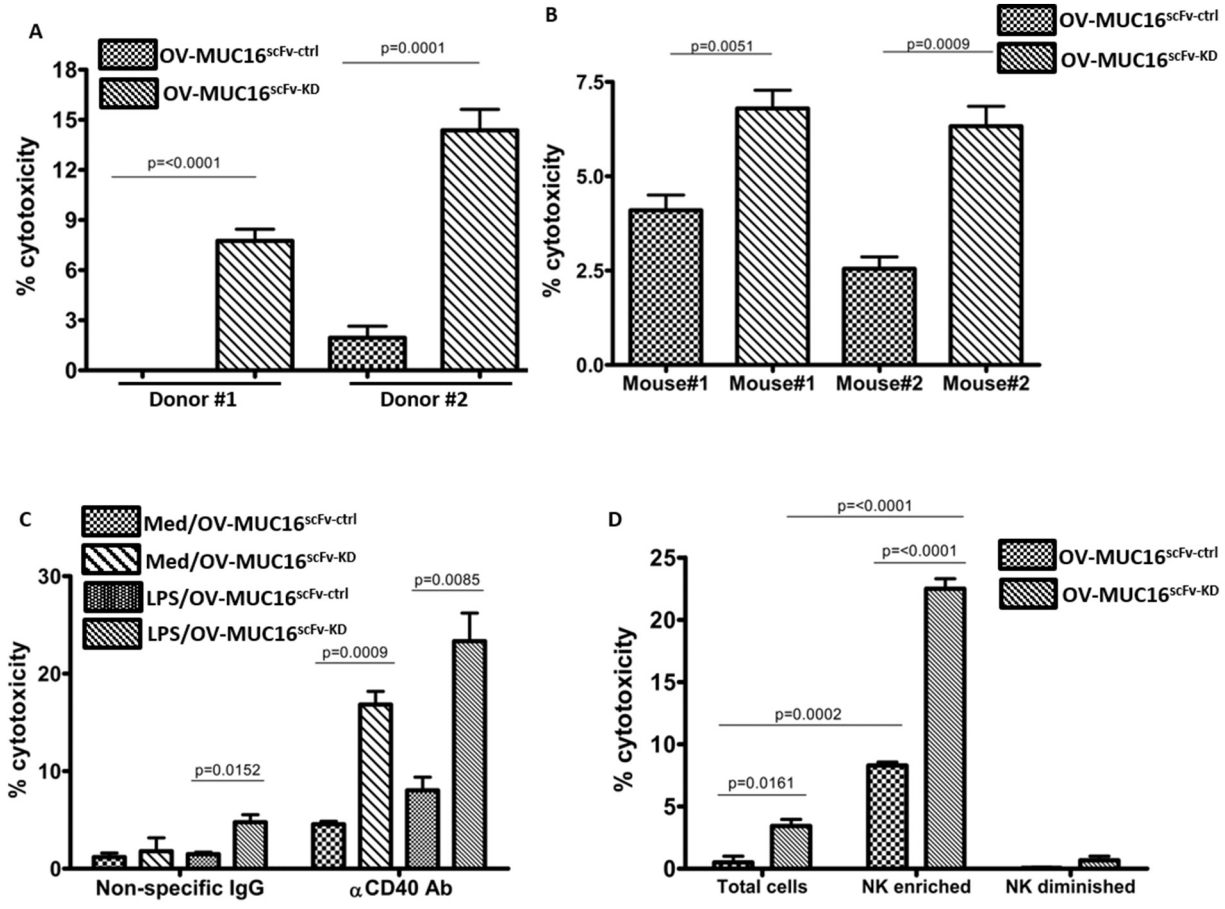

Fig. 4. Increased killing of OV-MUC16$^{scFv\text{-}KD}$ cells by murine NK cells. A: NK cell cytotoxicity assays were conducted using human peripheral blood mononuclear cells (PBMC) isolated from two healthy donors and ^{51}Cr-labeled OV-MUC16$^{scFv\text{-}ctrl}$ or OV-MUC16$^{scFv\text{-}KD}$ cells at effector:target cell ratio of 50:1. After a 4 h incubation, the amount of ^{51}Cr released in the media from the lysed target cells was determined. B: Splenocytes isolated from C57BL/6 mice treated with agonistic anti-CD40 antibody (FGK45.5) were used for *in vitro* cytotoxicity assays. Percent cytolysis of OV-MUC16$^{scFv\text{-}ctrl}$ and OV-MUC16$^{scFv\text{-}KD}$ targets is shown. C: Ability of splenocytes from SCID mice to lyse OV-MUC16$^{scFv\text{-}ctrl}$ and OV-MUC16$^{scFv\text{-}KD}$ targets is shown. SCID mice were injected with anti-CD40 antibody. Cytotoxicity assays were conducted in the presence or absence of LPS. Data shown is at an effector:target ratio of 20:1. Each data point is mean of four independent experiments. D: Splenocytes from FGK45.5 CD40-treated SCID mice were obtained. NK cells from the splenocytes were enriched. Cytotoxicity assays were conducted with the entire splenocyte fractions (total cells), NK cells incompletely isolated from the splenocytes (NK enriched), or with splenocytes depleted of NK cells (NK diminished). OV-MUC16$^{scFv\text{-}ctrl}$ or OV-MUC16$^{scFv\text{-}KD}$ cells were used as targets. For these cytotoxicity assays, a 20:1 effector:target cell ratio was used. Data is the average of triplicates.

(similarly stimulated with anti-CD40 antibody and LPS) also showed a 2.7-fold increase in the killing of OV-MUC16$^{scFv\text{-}KD}$ targets as compared to OV-MUC16$^{scFv\text{-}ctrl}$ cells, while cytolysis in the NK-diminished population was effectively eliminated (Fig. 4D).

3.4. MUC16 also protects ovarian cancer cells from murine macrophages

Next, we tested if MUC16 could also inhibit cytolytic responses by murine macrophages. The ability of murine macrophages to inhibit proliferation of human ovarian cancer cells was tested first in proliferation assays (Supplementary File 2). Peritoneal Exudate Cells (PEC) from FGK45.5 CD40-stimulated C57BL/6 mice inhibited the proliferation of B16 mouse melanoma cells as well as the human ovarian cancer cell line OVCAR-3. In this [^{3}H]-thymidine incorporation assay, since the macrophages are not proliferative, the increased [^{3}H]-thymidine uptake is a measure of proliferation of the tumor targets. Additional *in vitro* stimulation of the PECs with LPS resulted in further suppression of proliferation of both cell lines (Supplementary File 2).

Employing the [^{3}H]-thymidine incorporation assay, we observed that PEC from SCID mice inhibited the proliferation of OV-MUC16$^{scFv\text{-}KD}$ cells to a greater extent than the MUC16-expressing controls (Fig. 5A). Further confirmation of the increased ability of peritoneal macrophages to lyse OV-MUC16$^{scFv\text{-}KD}$ cells came from overnight cytotoxicity assays (Fig. 5B). PEC stimulated with LPS and IFN-γ showed approximately 3-fold increased cytotoxicity of OV-MUC16$^{scFv\text{-}KD}$ cells compared to OV-MUC16$^{scFv\text{-}ctrl}$ cells (Fig. 5B).

3.5. MUC16 knockdown increases Antibody Directed Cell-Mediated Cytotoxicity (ADCC) of ovarian cancer cells

The above experiments demonstrated that similarly to human NK cells, murine NK cells and macrophages were also able to lyse tumor targets with higher efficacy in the absence of MUC16. Additionally, our

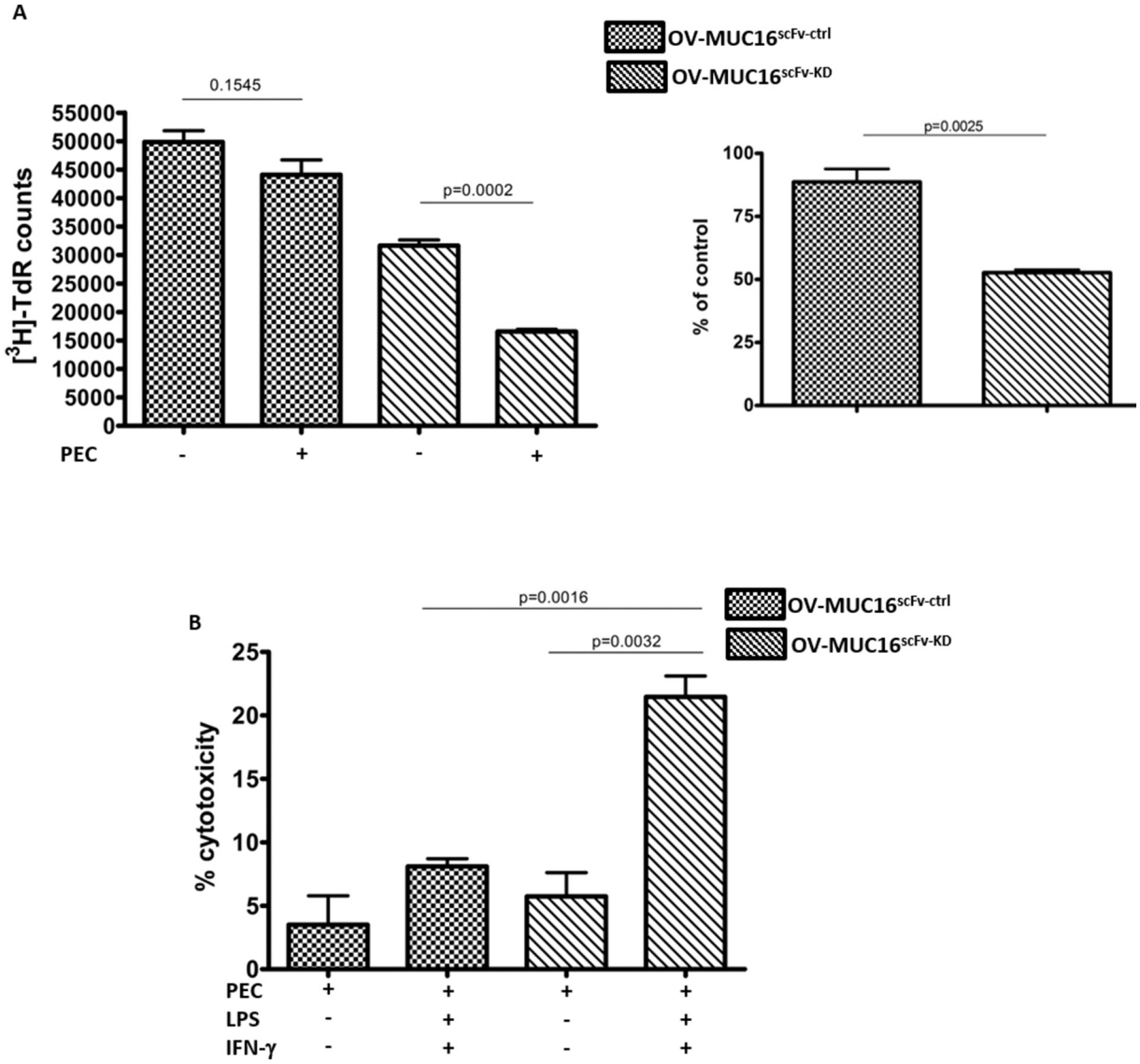

Fig. 5. Murine macrophages have an increased ability to inhibit proliferation and lyse OV-MUC16$^{scFv\text{-}KD}$ cells. A: PEC from SCID mice were used to determine the tumoristatic activity of unstimulated macrophages against OV-MUC16$^{scFv\text{-}ctrl}$ and OV-MUC16$^{scFv\text{-}KD}$ targets. Plastic-adherent PEC were incubated with the designated targets for 72 h and [^{3}H]-thymidine was added to the cells in the last 6 h of this assay. Tritium incorporation in the target cells was measured. Bar chart on the left shows non-normalized data and provides results on [^{3}H]-thymidine uptake cancer targets with and without PEC (effector cells). The bar chart on the right shows [^{3}H]-thymidine uptake data for the PEC-containing cultures in the bar chart on the left that are now normalized to the [^{3}H]-thymidine uptake observed in media-only controls (no PEC) of OV-MUC16$^{scFv\text{-}ctrl}$ and OV-MUC16$^{scFv\text{-}KD}$ targets. B: Plastic-adherent PEC from SCID mice were incubated with targets that were pre-labeled with ^{51}Cr at an effector:target ratio of 20:1 for 20 h. As indicated in the figure legends, the PEC were either maintained in culture media or in media containing either LPS, IFN-γ or both LPS and IFN-γ. Lysis of the target cells was determined by measuring the amount of ^{51}Cr released from the targets. Data shown in all plots in A and B is mean of four replicates.

results also showed that even after stimulation with LPS and IFN-γ, as well as a potent immunotherapeutic agent such as the anti-CD40 antibody, murine immune cells maintained better ability to attack MUC16-deficient cells than MUC16-expressing cells. This observation led us to investigate if immunotherapeutic agents that have been studied for the treatment of ovarian cancer may also be less effective when the tumor cells express MUC16 on their cell surface.

The murine antibody KS1/4 specifically recognizes Epithelial Cell Adhesion Molecule (EpCAM) [31,32]). The immunocytokine KSIL-2 is a fusion-protein of the humanized form of the KS1/4 murine monoclonal antibody and human IL-2 [33]. HuKSIL-2 has been tested as an immunotherapeutic agent for EpCAM-positive cancers in a Phase I clinical trial that included 15 women with recurrent ovarian cancer [32]. KSIL-2 is an activator of NK cell responses because it can induce target cell killing by ADCC and also increase NK-target synapse formation by engaging and polarizing IL2 receptors [34]. When lysis assays with murine splenocytes from FGK45.5 CD40-stimulated C57BL/6 mice were conducted in the presence of KS1/4, OV-MUC16$^{scFv\text{-}KD}$ cells were lysed approximately 1.5-fold more than OV-MUC16$^{scFv\text{-}ctrl}$ cells (Fig. 6A). Since the lysis assays were conducted over a four-hour period, the target cell killing observed is primarily due to NK cell activity.

The increase in ADCC of OV-MUC16$^{scFv\text{-}KD}$ was not due to increased binding of the KS1/4 antibody to these cells compared to OV-MUC16$^{scFv\text{-}ctrl}$ cells as determined by the surface binding of this antibody to the cells by flow cytometry (Fig. 6B). On the contrary, binding of KS1/4 to OV-MUC16$^{scFv\text{-}KD}$ cells was considerably lower than OV-MUC16$^{scFv\text{-}ctrl}$ cells (MFI 84.7 *vs* 380.6, respectively; Fig. 6B).

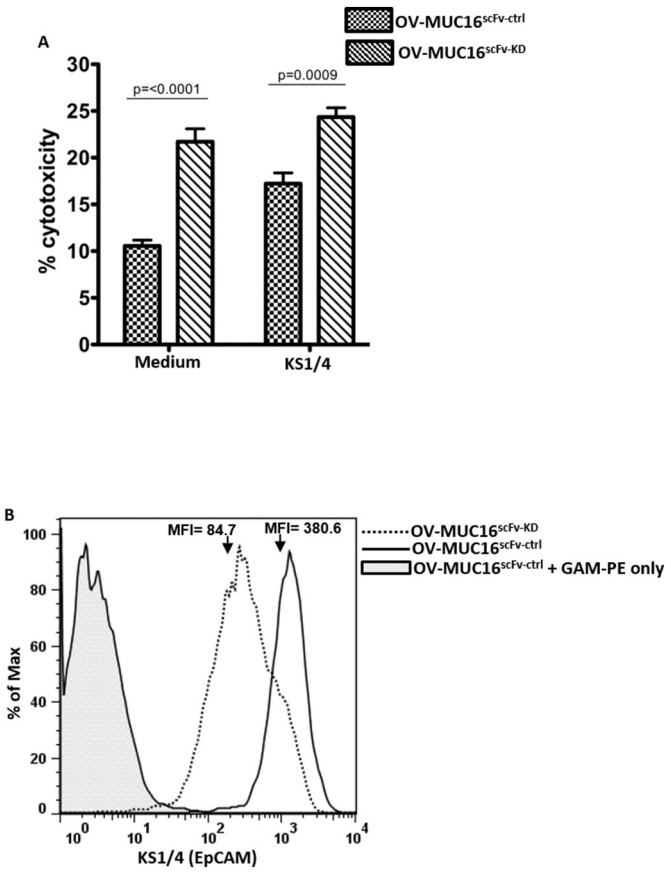

Fig. 6. MUC16 knockdown leads to increased susceptibility of ovarian cancer cells to ADCC. (A) Splenocytes from anti-CD40 antibody-treated C57BL/6 mice were used in ADCC assays to determine if their NK cells were able to lyse OV-MUC16$^{scFv\text{-}KD}$ cells and OV-MUC16$^{scFv\text{-}ctrl}$ cells in the presence or absence of KS1/4 antibody. (B) Flow cytometry was used to monitor the binding of KS1/4 antibody to OV-MUC16$^{scFv\text{-}ctrl}$ and OV-MUC16$^{scFv\text{-}KD}$ cells. Phycoerythrin-labeled goat anti-mouse secondary antibody was used for detection. Shaded histogram shows native binding of the secondary antibody. Data shown is representative of three independent assays.

4. Discussion

Our studies demonstrate that human MUC16 inhibits the cytolytic functions of murine NK cells and macrophages to a similar degree as the inhibition seen with human innate immune cells. These studies are important steps in using mouse models to delineate the immunoregulatory roles of MUC16 that provide immune protection to ovarian and other epithelial tumors. Several recent studies highlight the need to investigate the effects of MUC16 on immune cells. Most importantly, the correlation of decreased therapeutic responses of farletuzumab and amatuximab in patients with higher circulating levels of MUC16 (CA125) and the ability of this mucin to perturb interactions between therapeutic antibodies and Fc-γ receptors are raising the possibility that MUC16 and other mucins could influence the success of some anti-cancer immunotherapies. Our present study supports this apparent promiscuous ability of MUC16 to perturb potential monoclonal antibody-based immunotherapies, as all of our EpCAM-targeting treatments which we employed for immune stimulation (KS1/4 and KSIL-2, C215 antibody and its related immunocytokine, IC65) are adversely affected by the presence of MUC16.

MUC16, with its over 24,000 amino acids and extensive O– and N-linked glycan chains, may affect immune function *via* various mechanisms. Its physical structure could serve as an imposing size and charge barrier that prevents immune cells from forming synapses with tumors. Our glycomic analysis has revealed expression of sialylated Lewis^x and Lewis^y-terminated, bisecting type biantennary and other glycans that may influence immune cell function [35]. Elongation of O-linked glycans of MUC16 has also been suggested to suppress NK cell cytotoxicity [16]. Through its terminal α2–3-sialyl epitopes, MUC16 also engages the inhibitory immune cell receptor, Siglec-9 [13]. While these studies point to involvement of the MUC16 glycan chains in regulating immune responses, the effects of specific peptide regions of MUC16 interference with immune function have not been investigated. Full understanding of the immunoregulatory roles of a multifaceted molecule like MUC16 is going to require the use of diverse experimental tools with a significant role for mouse models. The demonstration that MUC16 also inhibits murine innate immune responses provides the foundation for such future studies.

In addition to its immunoregulatory roles, a growing body of evidence is also demonstrating that MUC16 enhances proliferation and metastasis of ovarian tumors [5,15,36,37]. It is already established that MUC16, by serving as a ligand of the GPI-linked glycoprotein mesothelin, promotes peritoneal metastasis of ovarian cancer cells [8,9,38–40]. Cell signaling occurring *via* the cytoplasmic tail of MUC16 promotes cancer cell growth [7]. Transfection of the MUC16 C-terminal tail in cell lines that do not express this mucin increases cell proliferation and also imparts resistance to cytotoxic effects of cisplatin [7,22]. More recent data further demonstrate that the knockdown of MUC16 causes cell cycle arrest in the G2/M phase and increases apoptosis in ovarian and breast cancer cell lines [10,41].

These non-immune functions of MUC16 are also intriguing and will require the use of mouse models for further scrutiny. Our demonstration that MUC16 can inhibit murine innate immune responses should advise caution when interpreting the non-immune effects of MUC16 in studies that employ mouse models. The effects of MUC16 observed in mouse studies focused on gauging the influence of this mucin on cancer cell proliferation and metastasis should be interpreted while taking into account its potential immunoregulatory roles and *vice versa*. As demonstrated by our studies, the resident NK cells or macrophages in SCID and SCID/Beige animals are competent in producing immune responses to tumors and hence the use of such "immunecompromised" models does not rule out the immunologic roles of MUC16.

Supplementary data to this article can be found online at https://doi.org/10.1016/j.ygyno.2018.12.023.

Conflict of interest disclosure statement

All of the co-authors declare that they do not have any relationships that could be construed as resulting in an actual, potential, or perceived conflict of interest with regard to the manuscript being submitted for review.

Acknowledgements

Funding for this research was provided by grants from the National Institutes of Health (1R21CA143616-01 and 1R41CA132520-01A2), Department of Defense (W81XWH-04-1-0102), and the Department of Obstetrics and Gynecology to MSP, charitable donation from Jean McKenzie, and research grants from the Wisconsin Ovarian Cancer Alliance to MSP and JPC. AR is supported by 1R01CA87025 from NCI. We are deeply grateful to Dagna Sheerar (University of Wisconsin-Madison Paul P. Carbone Comprehensive Cancer Center, Flow Cytometry Facility) for advice and assistance with the flow cytometry assays. We also acknowledge the support provided by the University of Wisconsin Comprehensive Cancer Centers Flow Cytometry facility which is supported by a core grant (CA14520) from the National Institutes of Health.

Author contributions

MF conducted all of the major experiments and helped in preparing the figures. AK, ALR, and XQ assisted with the flow cytometry and immunologic assays. MF and ALR also helped with writing of the manuscript. PMS and SDG were responsible for developing the immunocytokine reagents. JC and MSP designed the experiments and the overall study. MSP played a major role in writing the manuscript and developing the figures.

References

[1] M. Felder, A. Kapur, J. Gonzalez-Bosquet, S. Horibata, J. Heintz, R. Albrecht, et al., MUC16 (CA125): tumor biomarker to cancer therapy, a work in progress, Mol. Cancer 13 (2014) 129.
[2] T.J. O'Brien, J.B. Beard, L.J. Underwood, R.A. Dennis, A.D. Santin, L. York, The CA 125 gene: an extracellular superstructure dominated by repeat sequences, Tumour Biol. 22 (2001) 348–366.
[3] B.W. Yin, K.O. Lloyd, Molecular cloning of the ca125 ovarian cancer antigen. Identification as a new mucin, muc16, J. Biol. Chem. 276 (2001) 27371–27375.
[4] S. Das, S. Rachagani, M.P. Torres-Gonzalez, I. Lakshmanan, P.D. Majhi, L.M. Smith, et al., Carboxyl-terminal domain of MUC16 imparts tumorigenic and metastatic functions through nuclear translocation of JAK2 to pancreatic cancer cells, Oncotarget 6 (2015) 5772–5787.
[5] D. Haridas, M.P. Ponnusamy, S. Chugh, I. Lakshmanan, P. Seshacharyulu, S.K. Batra, MUC16: molecular analysis and its functional implications in benign and malignant conditions, FASEB J. 28 (2014) 4183–4199.
[6] K. Akita, M. Tanaka, S. Tanida, Y. Mori, M. Toda, H. Nakada, CA125/MUC16 interacts with Src family kinases, and over-expression of its C-terminal fragment in human epithelial cancer cells reduces cell-cell adhesion, Eur. J. Cell Biol. 92 (2013) 257–263.
[7] C. Theriault, M. Pinard, M. Comamala, M. Migneault, J. Beaudin, I. Matte, et al., MUC16 (CA125) regulates epithelial ovarian cancer cell growth, tumorigenesis and metastasis, Gynecol. Oncol. 121 (2011) 434–443.
[8] J.A. Gubbels, J. Belisle, M. Onda, C. Rancourt, M. Migneault, M. Ho, et al., Mesothelin-MUC16 binding is a high affinity, N-glycan dependent interaction that facilitates peritoneal metastasis of ovarian tumors, Mol. Cancer 5 (2006) 50.
[9] A. Rump, Y. Morikawa, M. Tanaka, S. Minami, N. Umesaki, M. Takeuchi, et al., Binding of ovarian cancer antigen CA125/MUC16 to mesothelin mediates cell adhesion, J. Biol. Chem. 279 (2004) 9190–9198.
[10] I. Lakshmanan, M.P. Ponnusamy, S. Das, S. Chakraborty, D. Haridas, P. Mukhopadhyay, et al., MUC16 induced rapid G2/M transition via interactions with JAK2 for increased proliferation and anti-apoptosis in breast cancer cells, Oncogene 31 (2012) 805–817.
[11] M.S. Patankar, J. Yu, J.C. Morrison, J.A. Belisle, F.A. Lattanzio, Y. Deng, et al., Potent suppression of natural killer cell response mediated by the ovarian tumor marker CA125, Gynecol. Oncol. 99 (2005) 704–713.
[12] J.A. Belisle, J.A. Gubbels, C.A. Raphael, M. Migneault, C. Rancourt, J.P. Connor, et al., Peritoneal natural killer cells from epithelial ovarian cancer patients show an altered phenotype and bind to the tumour marker MUC16 (CA125), Immunology (2007) 418–429.
[13] J.A. Belisle, S. Horibata, J.A. Gubbels, S. Petrie, A. Kapur, S. Andre, et al., Identification of Siglec-9 as the receptor for MUC16 on human NK cells, B cells, and monocytes, Mol. Cancer 9 (2010) 118.
[14] J.A. Gubbels, M. Felder, S. Horibata, J.A. Belisle, A. Kapur, H. Holden, et al., MUC16 provides immune protection by inhibiting synapse formation between NK and ovarian tumor cells, Mol. Cancer 9 (2010) 11.
[15] S. Das, P.D. Majhi, M.H. Al-Mugotir, S. Rachagani, P. Sorgen, S.K. Batra, Membrane proximal ectodomain cleavage of MUC16 occurs in the acidifying Golgi/post-Golgi compartments, Sci. Rep. 5 (2015) 9759.
[16] C.B. Madsen, K. Lavrsen, C. Steentoft, M.B. Vester-Christensen, H. Clausen, H.H. Wandall, et al., Glycan elongation beyond the mucin associated tn antigen protects tumor cells from immune-mediated killing, PLoS One 8 (2013), e72413.
[17] B.B. Menon, C. Kaiser-Marko, S. Spurr-Michaud, A.S. Tisdale, I.K. Gipson, Suppression of Toll-like receptor-mediated innate immune responses at the ocular surface by the membrane-associated mucins MUC1 and MUC16, Mucosal Immunol. 8 (2015) 1000–1008.
[18] J.B. Kline, R.P. Kennedy, E. Albone, Q. Chao, S. Fernando, J.M. McDonough, et al., Tumor antigen CA125 suppresses antibody-dependent cellular cytotoxicity (ADCC) via direct antibody binding and suppressed Fc-gamma receptor engagement, Oncotarget 8 (2017) 52045–52060.
[19] N.C. Nicolaides, C. Schweizer, E.B. Somers, W. Wang, S. Fernando, E.N. Ross, et al., CA125 suppresses amatuximab immune-effector function and elevated serum levels are associated with reduced clinical response in first line mesothelioma patients, Cancer Biol. Ther. 19 (2018) 622–630.
[20] W. Wang, E.B. Somers, E.N. Ross, J.B. Kline, D.J. O'Shannessy, C. Schweizer, et al., FCGR2A and FCGR3A genotypes correlate with farletuzumab response in patients with first-relapsed ovarian cancer exhibiting low CA125, Cytogenet. Genome Res. 48 (2017) 4509–4518.
[21] T.D. Blalock, S.J. Spurr-Michaud, A.S. Tisdale, S.R. Heimer, M.S. Gilmore, V. Ramesh, et al., Functions of MUC16 in corneal epithelial cells, Invest. Ophthalmol. Vis. Sci. 48 (2007) 4509–4518.
[22] M. Boivin, D. Lane, A. Piche, C. Rancourt, CA125 (MUC16) tumor antigen selectively modulates the sensitivity of ovarian cancer cells to genotoxic drug-induced apoptosis, Gynecol. Oncol. 115 (2009) 407–413.
[23] J.P. Connor, M. Felder, J. Hank, J. Harter, J. Gan, S.D. Gillies, et al., Ex vivo evaluation of anti-EpCAM immunocytokine huKS-IL2 in ovarian cancer, J. Immunother. 27 (2004) 211–219.
[24] S.D. Gillies, A new platform for constructing antibody-cytokine fusion proteins (immunocytokines) with improved biological properties and adaptable cytokine activity, Protein Eng. Des. Sel. 26 (2013) 561–569.
[25] T.L. Whiteside, Measurement of cytotoxic activity of NK/LAK cells, Curr. Protoc. Immunol. (1996) Chapter 7:Unit 7.18.
[26] A.L. Rakhmilevich, M.J. Baldeshwiler, T.J. Van De Voort, M.A. Felder, R.K. Yang, N.A. Kalogriopoulos, et al., Tumor-associated myeloid cells can be activated in vitro and in vivo to mediate antitumor effects, Cancer Immunol. Immunother. 61 (2012) 1683–1697.
[27] M. Comamala, M. Pinard, C. Theriault, I. Matte, A. Albert, M. Boivin, et al., Downregulation of cell surface CA125/MUC16 induces epithelial-to-mesenchymal transition and restores EGFR signalling in NIH:OVCAR3 ovarian carcinoma cells, Br. J. Cancer 104 (2011) 989–999.
[28] J.G. Turner, A.L. Rakhmilevich, L. Burdelya, Z. Neal, M. Imboden, P.M. Sondel, et al., Anti-CD40 antibody induces antitumor and antimetastatic effects: the role of NK cells, J. Immunol. 166 (2001) 89–94.
[29] G.L. Beatty, E.G. Chiorean, M.P. Fishman, B. Saboury, U.R. Teitelbaum, W. Sun, et al., CD40 agonists alter tumor stroma and show efficacy against pancreatic carcinoma in mice and humans, Science 331 (2011) 1612–1616.
[30] P. Conti, R.A. Dempsey, M. Reale, R.C. Barbacane, M.R. Panara, M. Bongrazio, et al., Activation of human natural killer cells by lipopolysaccharide and generation of interleukin-1 alpha, beta, tumour necrosis factor and interleukin-6. Effect of IL-1 receptor antagonist, Immunology 73 (1991) 450–456.
[31] M.S. Perez, L.E. Walker, Isolation and characterization of a cDNA encoding the KS1/4 epithelial carcinoma marker, J. Immunol. 142 (1989) 3662–3667.
[32] J.P. Connor, M.C. Cristea, N.L. Lewis, L.D. Lewis, P.B. Komarnitsky, M.R. Mattiacci, et al., A phase 1b study of humanized KS-interleukin-2 (huKS-IL2) immunocytokine with cyclophosphamide in patients with EpCAM-positive advanced solid tumors, BMC Cancer 13 (2013) 20.
[33] R. Xiang, H.N. Lode, C.S. Dolman, T. Dreier, N.M. Varki, X. Qian, et al., Elimination of established murine colon carcinoma metastases by antibody-interleukin 2 fusion protein therapy, Cancer Res. 57 (1997) 4948–4955.
[34] Gubbels J.A.A. GB, I.N. Buhtoiarov, S. Horibata, A.K. Kapur, D. Patel, J.A. Hank, S.D. Gillies, P.M. Sondel, J. Connor, M.S. Patankar, Ab-IL2 fusion proteins mediate NK cell immune synapse formation by polarizing CD25 to the target cell-effector cell interface, Cancer Immunol. Immunother. 60 (2011) 1789–1800.
[35] N. Kui Wong, R.L. Easton, M. Panico, M. Sutton-Smith, J.C. Morrison, F.A. Lattanzio, et al., Characterization of the oligosaccharides associated with the human ovarian tumor marker CA125, J. Biol. Chem. 278 (2003) 28619–28634.
[36] D. Haridas, S. Chakraborty, M.P. Ponnusamy, I. Lakshmanan, S. Rachagani, E. Cruz, et al., Pathobiological implications of MUC16 expression in pancreatic cancer, PLoS One 6 (2011), e26839.
[37] I. Lakshmanan, S. Salfity, P. Seshacharyulu, S. Rachagani, A. Thomas, S. Das, et al., MUC16 regulates TSPYL5 for lung cancer cell growth and Chemoresistance by suppressing p53, Clin. Cancer Res. 23 (2017) 3906–3917.

[38] B.K. Sathyanarayana, Y. Hahn, M.S. Patankar, I. Pastan, B. Lee, Mesothelin, Stereocilin, and Otoancorin are predicted to have superhelical structures with ARM-type repeats, BMC Struct. Biol. 9 (1) (2009).
[39] N. Scholler, B. Garvik, M. Hayden-Ledbetter, T. Kline, N. Urban, Development of a CA125-mesothelin cell adhesion assay as a screening tool for biologics discovery, Cancer Lett. 247 (2006) 130–136.
[40] L. Bergan, J.A. Gross, B. Nevin, N. Urban, N. Scholler, Development and in vitro validation of anti-mesothelin biobodies that prevent CA125/mesothelin-dependent cell attachment, Cancer Lett. 255 (2007) 263–274.
[41] S. Reinartz, S. Failer, T. Schuell, U. Wagner, CA125 (MUC16) gene silencing suppresses growth properties of ovarian and breast cancer cells, Eur. J. Cancer 48 (2011) 1558–1569.